Localized injection of miRNA-21-enriched extracellular vesicles effectively restores cardiac function after myocardial infarction

Yu Song[1*], Cheng Zhang[1,2*], Jinxiang Zhang[3*], Zhanying Jiao[1], Nianguo Dong[4#], Guobin Wang[2#], Zheng Wang[1,2#], Lin Wang[1,5#]

1. Research Center for Tissue Engineering and Regenerative Medicine, Union Hospital, Tongji Medical College, Huazhong University of Science and Technology, Wuhan, 430022, China
2. Department of Gastrointestinal Surgery, Union Hospital, Tongji Medical College, Huazhong University of Science and Technology, Wuhan, 430022, China
3. Department of Emergency Surgery, Union Hospital, Tongji Medical College, Huazhong University of Science and Technology, Wuhan, 430022, China
4. Department of Cardiovascular Surgery, Union Hospital, Tongji Medical College, Huazhong University of Science and Technology, Wuhan, 430022, China
5. Department of Clinical Laboratory, Union Hospital, Tongji Medical College, Huazhong University of Science and Technology, Wuhan, 430022, China

[*], These authors contributed equally to this work.

[#], Corresponding authors. Phone: 86-27-85726612, E-mail: lin_wang@hust.edu.cn (L. Wang); zhengwang@hust.edu.cn (Z. Wang); wgb@hust.edu.cn (G. Wang); dongnianguo@hotmail.com (N. Dong)

Table S1. Reverse transcription primers and real-time PCR primers.

miRNA/gene name	Primer name	Sequence (5'-3')
mmu-miR21-5p	Stem-loop RT	GTCGTATCCAGTGCAGGGTCCGAGGTATT CGCACTGGATACGACTCAACA
	forward	TGCTCGTAGCTTATCAGACTGATG
	reverse	CAGTGCAGGGTCCGAGGTAT
	cDNA	GTCGTATCCAGTGCAGGGTCCGAGGTATT CGCACTGGATACGACTCAACATCAGTCT GATAAGCTA
pre-miR21	forward	GTACCACCTTGTCGGATAGC
	reverse	TGTCAGACAGCCCATCGACT
pri-miR21	forward	TTGGCATTAAGCCCCAGCAA
	reverse	AGCCATGCGATGTCACGACC
U6	Stem-loop RT	GTCGTATCCAGTGCAGGGTCCGAGGTATT CGCACTGGATACGACAAAATA
	forward	GCTTCGGCAGCACATATACTAAAAT
	reverse	CGCTTCACGAATTTGCGTGTCAT
human GAPDH	forward	AAGGCTGTGGGCAAGG
	reverse	TGGAGGAGTGGGTGTCG
rat β-actin	forward	GGAGATTACTGCCCTGGCTCCTA
	reverse	GACTCATCGTACTCCTGCTTGCTG
mouse GAPDH	forward	ATGTTTGTGATGGGTGTGAA
	reverse	ATGCCAAAGTTGTCATGGAT

Table S2. The Number of study samples.

No. of Mice	Sham	MI	Ctrl-EVs	miR21-EVs
Total	9	20	20	23
Drop out	N/A	3	0	4
Death / cardiac rupture	0/0	8/2	9/0	5/0
Experimental analysis at 1 week after MI	3	3	3	4
Experimental analysis at 4 weeks after MI	6	6	8	10

Figure S1. Sequence alignment of conserved base pairs (red) between miR21 and 3'UTR of PDCD4 in different species as indicated.

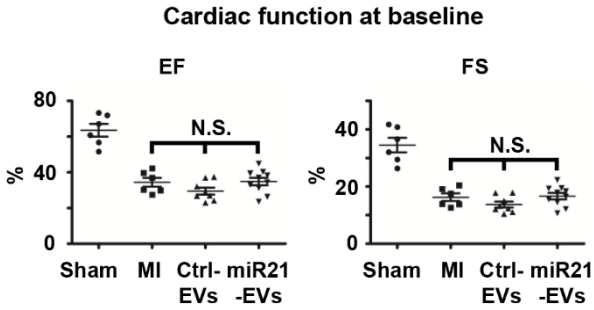

Figure S2. Effect of miR21-loaded EVs on the cardiac function of the infarcted hearts.

Ejection fraction (EF) and fractional shortening (FS) were measured by echocardiography at baseline (1 day post-MI) after sham operations (sham group) or MI treatment with the injection of PBS (MI group), Ctrl-EVs, and miR21-EVs. Data shown as mean ± SEM. N.S., no significant.

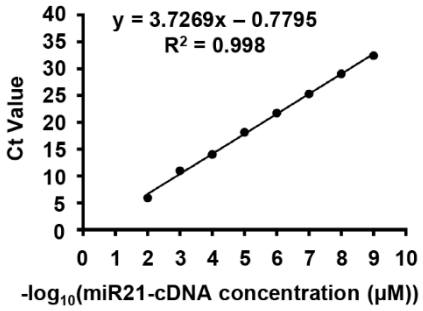

Figure S3. The standard curve of miR21 for the quantification of EV's miR21 using real-time PCR. The negative logarithms of the different miR21-cDNA concentrations (X axis) were plotted against the Ct values (Y axis). The linear regression equation and coefficient of determination were shown.

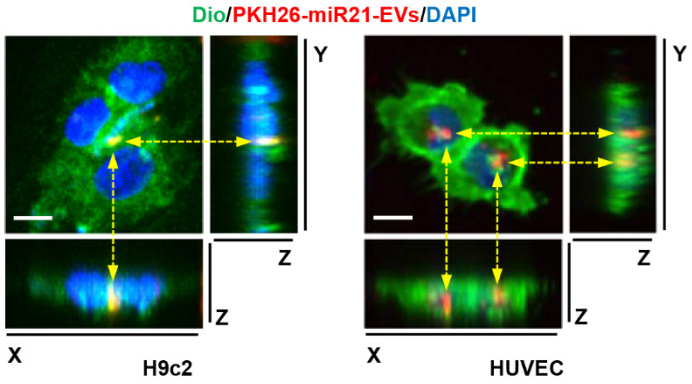

Figure S4. The 3D images of PKH26-labeled miR21-EVs uptaking by H9c2 cells and HUVECs. The lipophilic Dio dye (green) was used to label cell membrane. Z-stack images were acquired and corresponding 3D images were created by IMARIS software. The position of PKH26-miR21-EVs was indicated by yellow dashed arrows and observed from three perspectives, X-Y plane, X-Z plane and Y-Z plane. Scale bar, 10 μm.

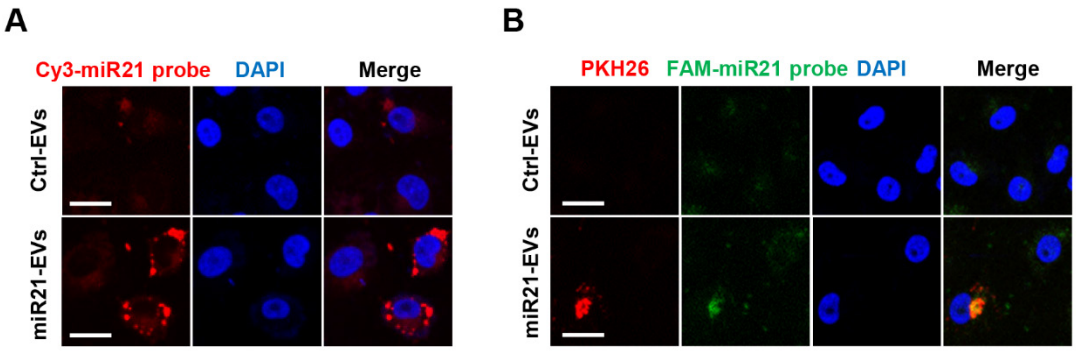

Figure S5. Detection of miR21 uptake by FISH analysis *in vitro*. Unlabeled (A) or PKH26-labeled EVs (B) (2 μg/mL) were added in HUVECs respectively. After being incubated at 37 °C with 5% CO_2 for 4 h, hybridization with Cy3 labeled (A, red color) or FAM labeled (B, green color) miR21 oligonucleotide probe (8 ng/μL) was carried out. Scale bar, 20 μm.

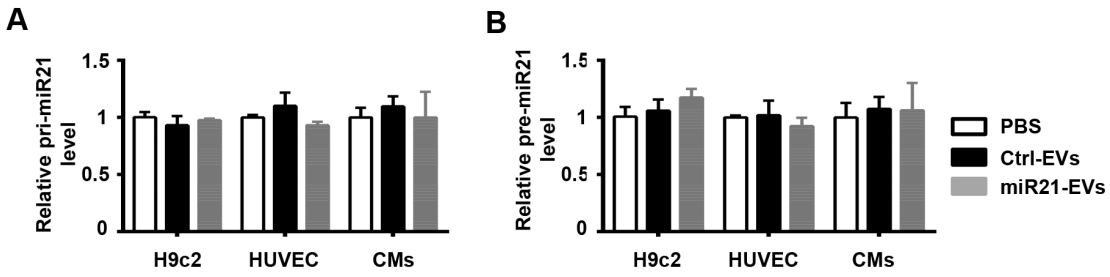

Figure S6. Analysis of pri-miR21 and pre-miR21 levels in H9c2 cells, HUVECs and CMs by qPCR. Cells were incubated with PBS, Ctrl-EVs or mi21-EVs (2 μg/mL), respectively, for 12 h. For comparison, the levels of pri- and pre-miR21 in PBS group were set as 1. Data shown as mean ± SEM.

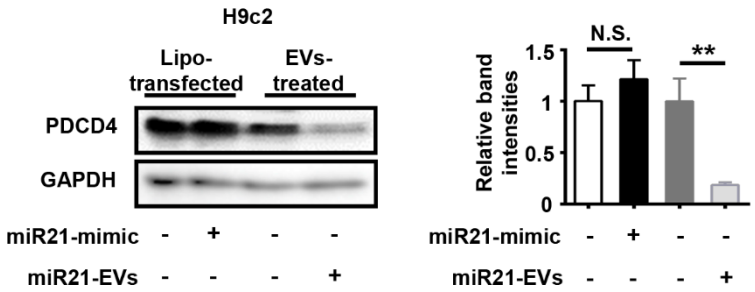

Figure S7. Comparison of inhibitory efficiency of PDCD4 between EVs and liposomes.

H9c2 cells were treated with miR21-EVs (2 μg/mL) or transfected with miR21-mimic (10nM) by Lipofectamine 2000 for 12 h. PDCD4 protein level was determined by Western blot analysis. The ratio of PDCD4 to GAPDH (relative band intensity) was measured using the Image-Pro Plus software. Data shown as mean ± SEM. **, $p < 0.01$, N.S., no significant.

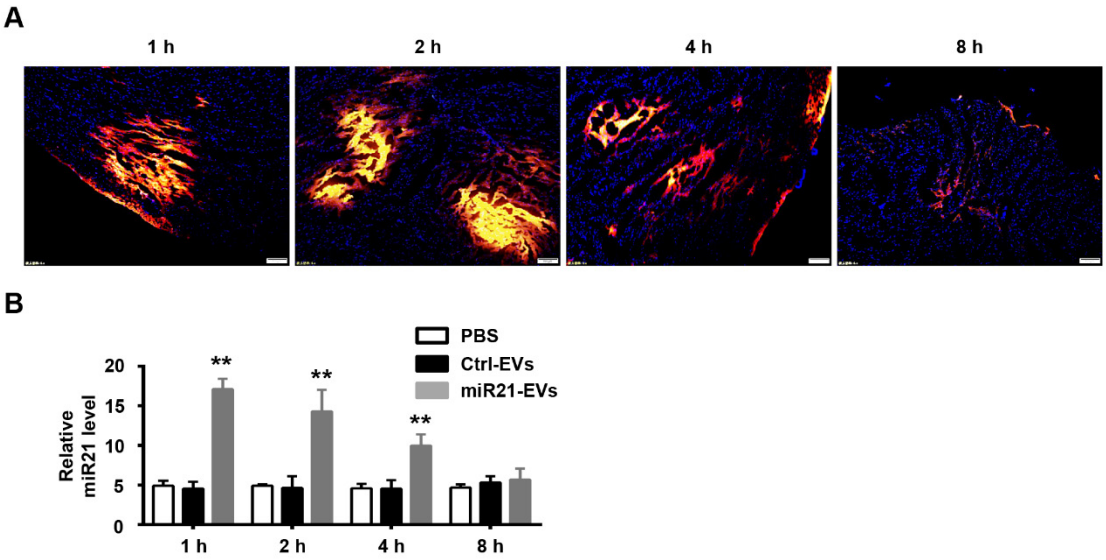

Figure S8. Distribution of miR21-EVs and the expression level of miR21 in infarcted myocardium of MI mice. (A) Fluorescent microscopy images of miR21-EVs' distribution in infarcted myocardium of mice. MiR21-EVs were labeled with red fluorescent dye PKH26 and injected into the infarct hearts of MI mice for indicated time (20 μg EVs per mouse). Scale bar, 100 μm. (B) Relative miR21 expression level in infarcted LV myocardium at 1, 2, 4 and 8 hours post injection by qPCR. Data shown as mean ± SEM. **, $p < 0.01$.

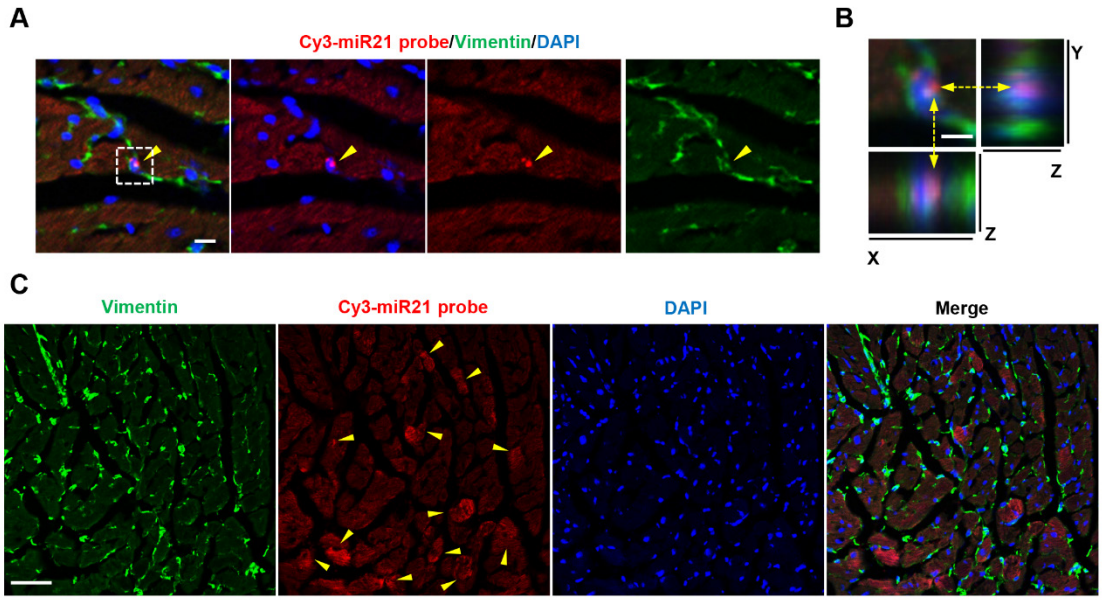

Figure S9. Distribution of miR21 in cardiac fibroblasts of infarcted mouse heart. (A) Cell-specific FISH analysis in infarcted LV myocardium of mice. MiR21-EVs (20 μg) were injected into the infarct hearts of mice for 1 hour. Cardiac fibroblasts were stained with anti-Vimentin (green). Cy3-miR21 probe (red) was used to detect miR21. Concentrated miR21 was indicated by yellow arrowheads. Scale bar, 10 μm. (B) The 3D images of corresponding white dashed box of (A). The position of Cy3-miR21 probe was indicated by yellow dashed arrows and observed from three perspectives, X-Y plane, X-Z plane and Y-Z plane. Scale bar, 5 μm. (C) Comparison of miR21-EVs' uptake efficiency between cardiomyocytes and fibroblasts. Infarcted mouse heart was treated as described above. The strongly miR21-positive cardiomyocytes were indicated by yellow arrowheads. There is no exogenous miR21 internalized in fibroblasts in this field. Scale bar, 50 μm.

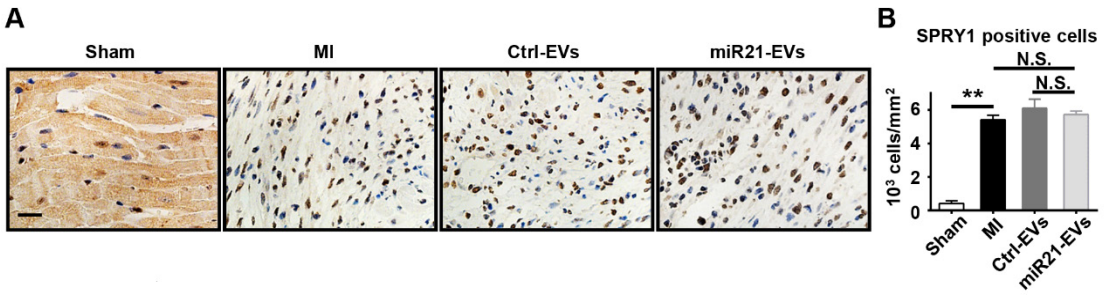

Figure S10. Effect of miR21-loaded EVs on the SPRY1 expression of the infarcted hearts.

(A) The representative immunohistochemistry images show SPRY1 positive cells in the peri-infarct zone of the myocardial sections of MI group or EVs-injected groups 1 week after MI. For sham group, the image of left ventricular were selected. Scale bars, 20 μm. (B) Quantification of SPRY1 positive cells of the corresponding images of (A) (4 random fields per animal; n = 3, 3, 3, and 4 for sham group, MI group, Ctrl-EVs group, and miR21-EVs group, respectively). Data shown as mean ± SEM. **, $p < 0.01$, N.S., no significant.

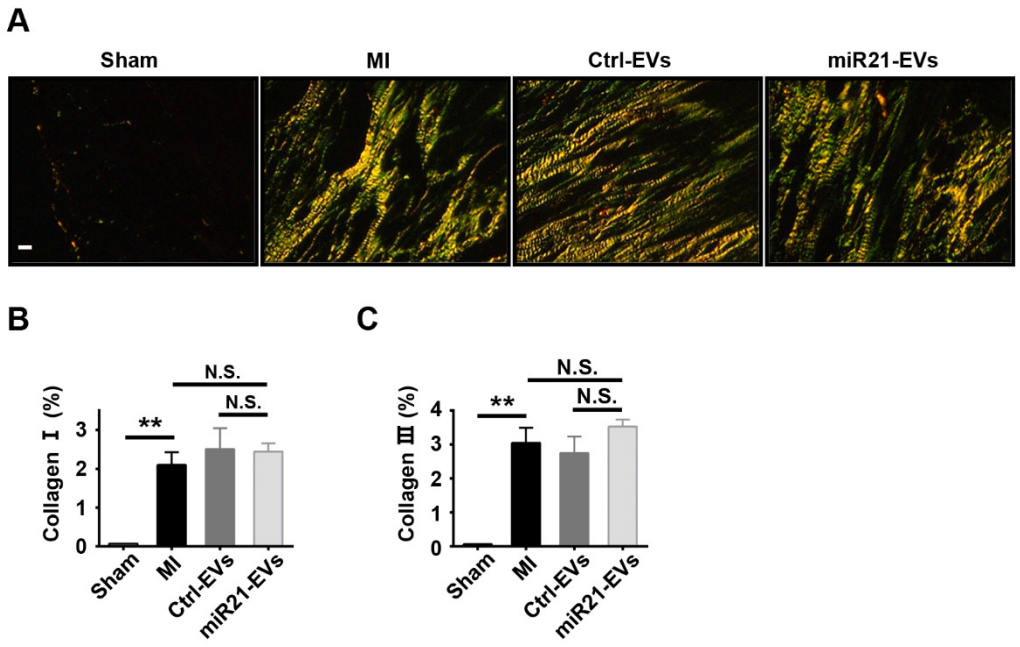

Figure S11. **Effect of miR21-loaded EVs on collagen content of the infarcted hearts.** (A) The representative polarized images show collagen fibers in the peri-infarct areas of the myocardial sections of MI group or EVs-injected groups 4 week after MI. For sham group, the image of left ventricular were selected. The yellow, orange or red color indicates the type I collagen, and the green color indicates collagen III. Scale bars, 20 μm. (B and C) Quantification of collagen I (B) and collagen III (C) of the corresponding images of (A) (4 random fields per animal; n = 3, 4, 4, and 5 for sham group, MI group, Ctrl-EVs group, and miR21-EVs group, respectively). Data shown as mean ± SEM. **, $p < 0.01$, N.S., no significant.

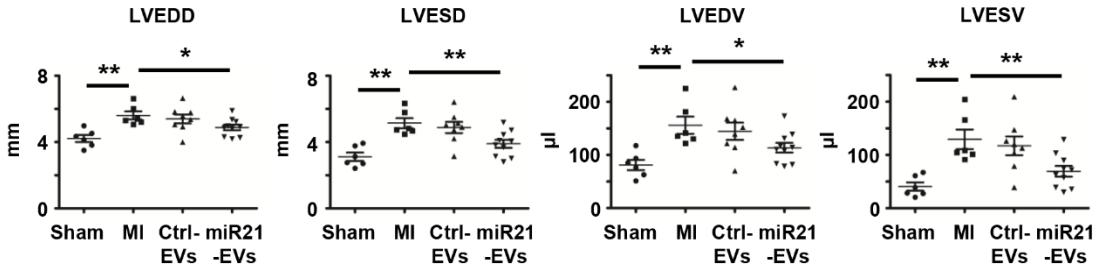

Figure S12. Examination of cardiac function by echocardiography. Left ventricular end-diastolic dimension (LVEDD), left ventricular end-systolic dimension (LVESD), left ventricular end-diastolic volumes (LVEDV), and left ventricular end-systolic volumes (LVESV) were measured by echocardiography 4 weeks after sham operations (sham group) or MI treatment with the injection of PBS (MI group), Ctrl-EVs, and miR21-EVs. Data shown as mean ± SEM. **, $p < 0.01$, *, $p < 0.05$.

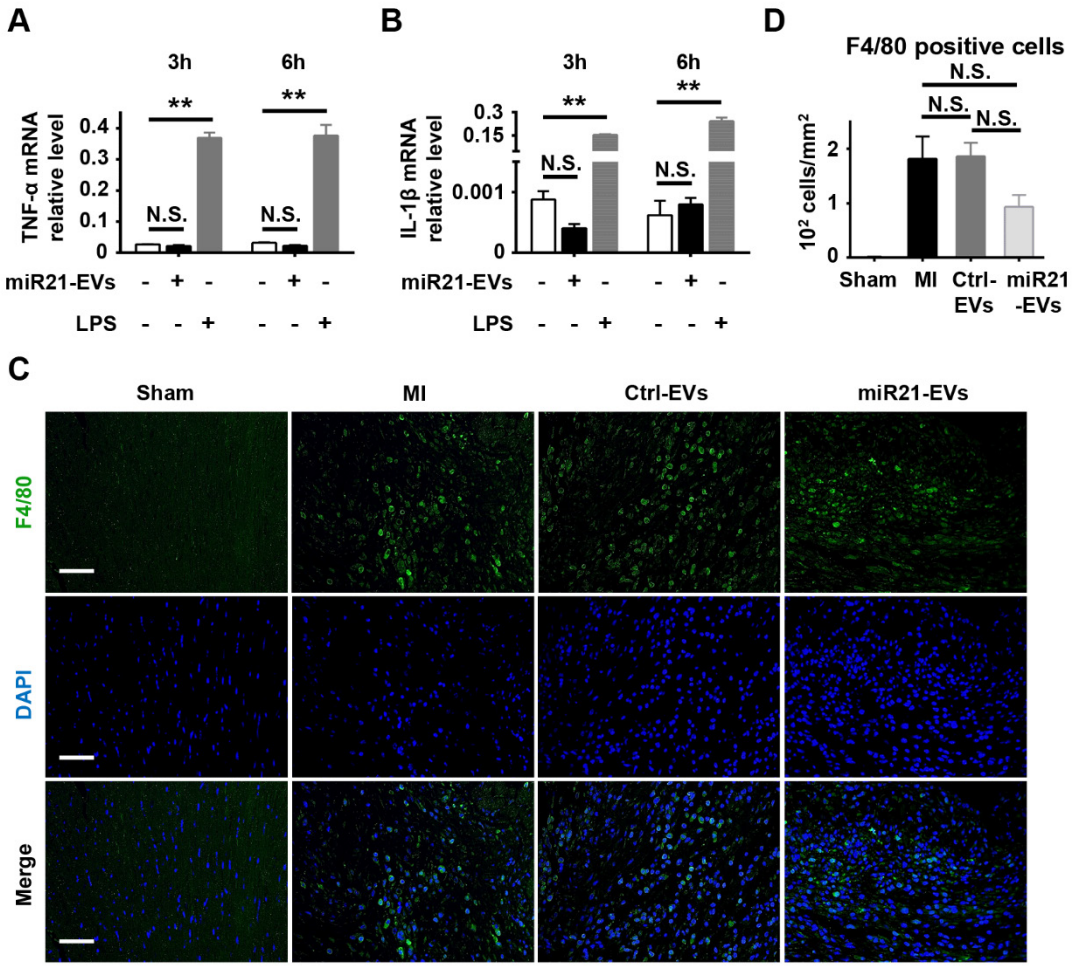

Figure S13. Effect of miR21-loaded EVs on inflammation *in vitro* and *in vivo*. (A-B) Quantification of mRNA levels of the two pro-inflammatory cytokines, TNF-a (A) and IL-1β (B), in Raw264.7 mouse macrophages that were incubated with miR21-EVs (2 μg/mL) for indicated time. The cells without any treatments were used as the negative control. LPS (100 ng/mL) was used to elicit an experimental inflammation response *in vitro*. (C) The representative immunofluorescence images show the infiltration of $F4/80^+$ macrophages at the peri-infarct zone of the animals of MI group, Ctrl-EVs group or miR21-EVs group 1 week after MI. For sham group, the image of left ventricular were selected. Scale bars, 50 μm. (D) Quantification of $F4/80^+$ macrophage density of (C) (4 random fields per animal; n = 3, 3, 3, and 4 for sham group, MI group, Ctrl-EVs group, and miR21-EVs group, respectively). Data

shown as mean ± SEM. **, $p < 0.01$, N.S., no significant.